

# UCSF

## UC San Francisco Previously Published Works

### Title

Effect of elevation of vascular endothelial growth factor level on exacerbation of hemorrhage in mouse brain arteriovenous malformation.

### Permalink

<https://escholarship.org/uc/item/14q259wp>

### Journal

Journal of Neurosurgery, 132(5)

### ISSN

0022-3085

### Authors

Cheng, Philip  
Ma, Li  
Shaligram, Sonali  
[et al.](#)

### Publication Date

2020

### DOI

10.3171/2019.1.jns183112

Peer reviewed

## Effect of elevation of vascular endothelial growth factor level on exacerbation of hemorrhage in mouse brain arteriovenous malformation

\*Philip Cheng, BA,<sup>1</sup> Li Ma, MD, PhD,<sup>1,2</sup> Sonali Shaligram, PhD,<sup>1</sup> Espen J. Walker, PhD,<sup>1</sup> Shun-Tai Yang, MD,<sup>1</sup> Chaoliang Tang, MD,<sup>1</sup> Wan Zhu, PhD,<sup>1</sup> Lei Zhan, RN,<sup>1</sup> Qiang Li, MD, PhD,<sup>1,3</sup> Xiaonan Zhu, MD,<sup>1</sup> Michael T. Lawton, MD,<sup>3</sup> and Hua Su, MD<sup>1</sup>

<sup>1</sup>Department of Anesthesia and Perioperative Care, Center for Cerebrovascular Research, University of California, San Francisco, California; <sup>2</sup>Department of Neurosurgery, Beijing Tiantan Hospital, Capital Medical University, Beijing, People's Republic of China; and <sup>3</sup>Department of Neurological Surgery, University of California, San Francisco, California

**OBJECTIVE** A high level of vascular endothelial growth factor (VEGF) has been implicated in brain arteriovenous malformation (bAVM) bleeding and rupture. However, direct evidence is missing. In this study the authors used a mouse bAVM model to test the hypothesis that elevation of focal VEGF levels in bAVMs exacerbates the severity of bAVM hemorrhage.

**METHODS** Brain AVMs were induced in adult mice in which activin receptor–like kinase 1 (*Alk1*, a gene that causes AVM) gene exons 4–6 were floxed by intrabasal ganglia injection of an adenoviral vector expressing Cre recombinase to induce *Alk1* mutation and an adeno-associated viral vector expressing human VEGF (AAV-VEGF) to induce angiogenesis. Two doses of AAV-VEGF ( $5 \times 10^9$  [high] or  $2 \times 10^9$  [low]) viral genomes were used. In addition, the common carotid artery and external jugular vein were anastomosed in a group of mice treated with low-dose AAV-VEGF 6 weeks after the model induction to induce cerebral venous hypertension (VH), because VH increases the VEGF level in the brain. Brain samples were collected 8 weeks after the model induction. Hemorrhages in the bAVM lesions were quantified on brain sections stained with Prussian blue, which detects iron deposition. VEGF levels were quantified in bAVM tissue by enzyme-linked immunosorbent assay.

**RESULTS** Compared to mice injected with a low dose of AAV-VEGF, the mice injected with a high dose had higher levels of VEGF ( $p = 0.003$ ) and larger Prussian blue–positive areas in the bAVM lesion at 8 or 9 weeks after model induction ( $p = 0.002$ ). VH increased bAVM hemorrhage in the low-dose AAV-VEGF group. The overall mortality in the high-dose AAV-VEGF group was 26.7%, whereas no mouse died in the low-dose AAV-VEGF group without VH. In contrast, VH caused a mortality of 50% in the low-dose AAV-VEGF group.

**CONCLUSIONS** Using mouse bAVM models, the authors provided direct evidence that elevation of the VEGF level increases bAVM hemorrhage and mouse mortality.

<https://thejns.org/doi/abs/10.3171/2019.1.JNS183112>

**KEYWORDS** brain hemorrhage; brain arteriovenous malformations; vascular endothelial growth factor; activin receptor–like kinase 1; venous hypertension; mouse model; vascular disorders

**T**HE rupture of a brain arteriovenous malformation (bAVM) is unpredictable, life threatening, and may result in long-term disability.<sup>12</sup> Existing methods for preventive eradication of bAVMs include microsurgical resection, radiosurgery, or embolization, often multimod-

al. Each of these treatment modalities carries a nontrivial rate of procedural complications, although the mortality rate varies among hospitals.<sup>1,10,28</sup> With the advancement of imaging techniques, more patients with asymptomatic bAVM will be diagnosed. The treatment of asymptomat-

**ABBREVIATIONS** AAV = adeno-associated viral vector; Ad-Cre = adenoviral vector expressing Cre recombinase; Ad-GFP = adenoviral vector expressing green fluorescent protein; bAVM = brain arteriovenous malformation; CCA = common carotid artery; EJV = external jugular vein; IACUC = Institutional Animal Care and Use Committee; UCSF = University of California, San Francisco; VEGF = vascular endothelial growth factor; VH = venous hypertension; WT = wild type.

**SUBMITTED** November 5, 2018. **ACCEPTED** January 18, 2019.

**INCLUDE WHEN CITING** Published online April 26, 2019; DOI: 10.3171/2019.1.JNS183112.

\* P.C. and L.M. contributed equally to this work.

ic patients has become increasingly controversial because the natural history for these patients may be less morbid than for those undergoing invasive therapies.<sup>10,11,26–28,34</sup> There is currently no specific medical therapy available to patients with bAVM.

Vascular endothelial growth factor (VEGF) is involved in normal and pathological angiogenesis.<sup>2,33</sup> The level of VEGF is abnormally high in resected bAVM tissue,<sup>17–22,36</sup> which may increase blood-brain barrier permeability and bAVM hemorrhage.<sup>18,31,41</sup> However, the association of high VEGF level and bAVM hemorrhage is suggested in the analysis of surgical specimens and patients' blood. The causal effect of VEGF levels on bAVM hemorrhage could not be proven using these methods, because surgery and vascular rupture can also increase VEGF expression.

The abnormal vessels in human bAVMs are exposed to variable degrees of increased intraluminal flow and venous hypertension (VH). We showed previously that VH created by anastomosis of the common carotid artery (CCA) with the external jugular vein (EJV) increases VEGF levels in the brains of mice and rats.<sup>13,40,44</sup>

In this study, we tested our hypothesis that an increase of VEGF level in the brains of mice that have an AVM-causing gene mutation increases bAVM hemorrhage. We investigated this through increase of the dose of the adeno-associated viral vector expressing VEGF (AAV-VEGF) at the time of bAVM phenotype induction<sup>38</sup> or through induction of VH 6 weeks after bAVM model induction.

## Methods

### Animals and Experimental Groups

The experimental protocols involving animal usage were approved by the Institutional Animal Care and Use Committee (IACUC) of the University of California, San Francisco (UCSF), and conformed to NIH guidelines. The staff of the Animal Core Facility and the IACUC of UCSF provided animal husbandry under the guidance of supervisors who are certified Animal Technologists, and IACUC faculty members and veterinary residents located on the Zuckerberg San Francisco General Hospital campus provided veterinary care.

Adult (8- to 10-week-old) *Alk1<sup>fl/fl</sup>* mice (*Alk1* [activin receptor-like kinase 1] exons 4–6 flanked by loxP sites)<sup>29</sup> in C57BL/6J background were used. Brain AVM was induced by coinjection of an adenoviral vector expressing Cre recombinase (Ad-Cre;  $2 \times 10^7$  plaque-forming units) to delete the *Alk1* gene and of AAV-VEGF to induce brain angiogenesis. Two doses of AAV-VEGF were used: 1) low dose:  $2 \times 10^9$  viral genomes; and 2) high dose:  $5 \times 10^9$  viral genomes. Our previous studies showed that the low-dose AAV-VEGF is sufficient to induce AVM formation in *Alk1*-deleted mouse brains.<sup>6,38</sup> A higher dose of AAV-VEGF was used here to test the impact of elevation of VEGF on bAVM hemorrhage. AAV-VEGF was prepared as described previously.<sup>30,35</sup> Ad-Cre virus was purchased from Vector Biolabs. Brain samples were collected 8 weeks after the viral vector injection; our previous study showed that the bAVMs are fully developed 8 weeks after model induction.<sup>38</sup>

TABLE 1. Experimental groups

Mouse Group	Viral Vector Injected		
	Ad-Cre	AAV-VEGF	VH
1	+	High dose	No
2	+	Low dose	No
3	+	Low dose	Sham VH
4	+	Low dose	Yes
5	–*	Low dose	Yes
6	+	AAV-LacZ	Yes

Mice in all groups were *Alk1<sup>20/2f</sup>* (2 alleles of *Alk1* were flanked by loxP sites).

\* Mice injected with Ad-GFP, an Ad-Cre control vector.

Mice were randomly assigned to 6 groups (Table 1), as follows: 1) injected with Ad-Cre and high-dose AAV-VEGF (45 mice); 2) injected with Ad-Cre and low-dose AAV-VEGF (20 mice); 3) injected with Ad-Cre and low-dose AAV-VEGF, and then subjected to sham VH (explored CCA and EJV) (6 mice); 4) injected with Ad-Cre and low-dose AAV-VEGF, and then subjected to VH (6 mice); 5) injected with adenoviral vector expressing green fluorescent protein (Ad-GFP) and low-dose AAV-VEGF, and then subjected to VH (6 mice); or 6) injected with Ad-Cre and low-dose AAV-LacZ, and then subjected to VH (5 mice). In addition, we also collected brains from 4 normal mice for control in the analysis of VEGF level in the brain (Fig. 1). For the VH study, we randomly assigned mice injected with Ad-Cre and low-dose AAV-VEGF into VH and non-VH groups 6 weeks after model induction.

### Stereotactic Injection of Viral Vectors

After being anesthetized with 2% isoflurane inhalation, the mice were placed in a stereotactic frame with a holder (David Kopf Instruments). A burr hole was drilled in the pericranium 2 mm lateral to the sagittal suture and 1 mm posterior to the coronal suture. Two microliters of

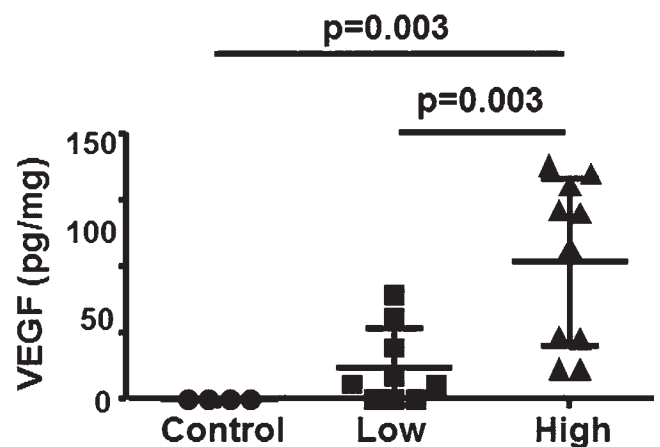


FIG. 1. An increase of AAV-VEGF dose increased VEGF protein in the brain. Control, uninjected brain; Low, mice injected with low-dose AAV-VEGF; High, mice injected with high-dose AAV-VEGF. There were 4 mice in the control group, 9 in the low-dose AAV-VEGF group, and 10 in the high-dose AAV-VEGF group.

viral suspension containing  $2 \times 10^7$  plaque-forming units of Ad-Cre or Ad-GFP and  $5 \times 10^9$  (high-dose) or  $2 \times 10^9$  (low-dose) viral genomes of AAV-VEGF or  $2 \times 10^9$  viral genomes of AAV-LacZ was stereotactically injected into the right basal ganglia at a rate of 0.2  $\mu$ l/min. The needle was withdrawn 10 minutes after the injection was finished. The wound was closed with a suture.

### Venous Hypertension

VH was created in mice 6 weeks after viral vector injection (induction of bAVM phenotype) by using the method described in our previous paper.<sup>40</sup> Briefly, after the mice were anesthetized with inhalation of 2% isoflurane, the right proximal CCAs were sutured to the right distal EJVs through an anterior (“ventral” in animals) midline cervical incision.

The sagittal sinus pressure was measured 1 day after the anastomosis of CCA and EJV. Through a scalp incision made in the midline over the sagittal suture, the parietal skull overlying the sagittal sinus was thinned using a drill. The sagittal sinus pressure was then measured by cannulating the sagittal sinus with a 36-gauge Nanofil needle connected to a pressure transducer and signal amplifier (PowerLab).

### ELISA

Brain tissues (1 mm<sup>3</sup>) containing the vector injection site were collected as described previously<sup>43</sup> and lysed in a cell lysis buffer (R&D Systems) and phenylmethylsulfonate (Cell Signaling). The protein concentrations were measured using Bradford reagents (Bio-Rad). Protein (1 mg) was used to quantify human VEGF expression by using a Quantikine ELISA kit (R&D Systems) because the AAV-VEGF vector that we have used in this study expresses human VEGF, and the sample was analyzed according to the manufacturer’s instructions.

### Lectin Perfusion

After mice were anesthetized using 2% isoflurane inhalation, 100  $\mu$ l of fluorescent *Lycopersicon esculentum* (tomato) lectin or DyLight 488 or DyLight 594 (Vector Laboratory) was injected into the EJV and allowed to circulate for 20 minutes. The mouse was then intracardially perfused with phosphate-buffered saline containing heparin (1 U/ml) to remove blood in the vessels. The brain was snap-frozen with dry ice and stored at  $-80^\circ\text{C}$ .

### Quantification of Vessel Densities and Dysplastic Vessels

Brains were cut into 20- $\mu$ m-thick coronal sections with a Leica RM2155 Microtome (Leica Microsystems). For the low-dose AAV-VEGF group, 2 sections, 0.5 mm rostral and 0.5 mm caudal to the needle track, were selected for vessel quantification. For the high-dose AAV-VEGF group, due to severe hemorrhage we had to select the 2 sections 0.7 to 0.9 mm rostral and caudal to the needle track for vessel quantification. Sections were coverslipped with Vectashield mounting medium containing DAPI (Vector Laboratories), which stains cell nuclei. Three areas (to the right, to the left, and below the injection site) within the angiogenic region of each section were imaged

under a  $\times 20$  microscopic objective lens. Vessel density was quantified using NIH Image 1.63 software and reported as mean vessel counts/mm<sup>2</sup>. The dysplasia index (number of vessels larger than 15  $\mu$ m in diameter per 200 vessels) was calculated as previously described.<sup>8,9,16,38</sup>

### Quantification of Hemorrhage

Two sections per brain, selected as described above, were used for the detection of iron deposition. An iron staining kit (Prussian blue stain, Sigma-Aldrich) was used. Slides were incubated in freshly prepared working iron stain solution for 10 minutes, washed in distilled water, and then counterstained with pararosaniline solution for 3 minutes. The area with positive staining (blue) was quantified using NIH Image 1.63 software. Data are presented as the percentage of blue-positive area in the entire hemisphere or pixels/hemisphere.

### Statistical Analyses

The quantification was done by researchers who were blinded to the treatment groups. Data are presented as the mean  $\pm$  SD. Due to the skewed nature of the Prussian blue-positive area, the data observations were log-transformed prior to the analysis. GraphPad Prism 6 was used for data analysis. One-way ANOVA was used to determine statistical significance among multiple groups, followed by pairwise multiple comparisons using the post hoc Tukey test. Fisher exact probability test was used for dichotomous variables comparing mortalities between groups. Statistical significance was set at  $p < 0.05$ . Sample sizes are indicated in the figure legends.

## Results

### High-Dose AAV-VEGF Elevated VEGF Level in Brain Tissue Around the Vector Injection Sites

To determine if an increase of the AAV-VEGF dose raised the VEGF level in the brain, brain tissues around vector injection sites were collected 8 weeks after the vector injection. VEGF levels were quantified using ELISA. Because the AAV-VEGF that we used expresses human VEGF<sub>165</sub>, we used a human VEGF Quantikine ELISA kit, and we did not detect any human VEGF in control mice that did not receive AAV-VEGF injection. Compared to low-dose AAV-VEGF-injected mice ( $18 \pm 21.9$  pg/mg brain tissue), mice injected with high-dose AAV-VEGF expressed a significantly higher VEGF protein ( $78 \pm 47.5$  pg/mg;  $p = 0.003$ , Fig. 1). Therefore, the high AAV-VEGF dose increased VEGF level in the brain.

### Vascular Structures Around the Vector Injection Sites Were Severely Damaged in Mice Treated With High-Dose AAV-VEGF

Vascular structures were severely damaged at the vector injection sites of the high-dose AAV-VEGF group (Fig. 2A). Unlike in the low-dose group, we had to select sections farther away from the needle tracks, which had less vascular damage, for performing vessel quantification. We were not able to detect the differences in vessel densities between the high-dose ( $1099 \pm 191.2/\text{mm}^2$ ) and low-dose ( $1141 \pm 188.9/\text{mm}^2$ ) AAV-VEGF groups with the sections

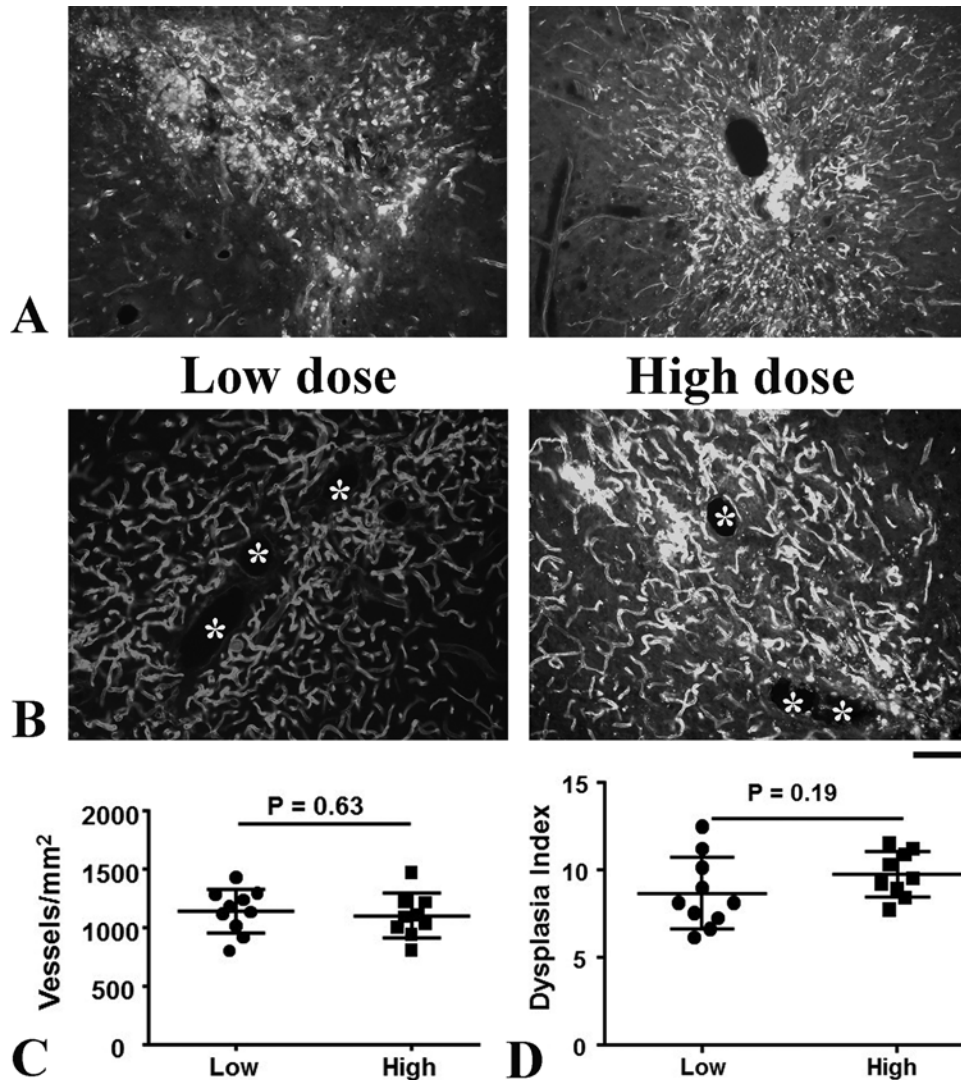


**FIG. 2.** Vascular structures were severely damaged near the needle track in mice that received high-dose AAV-VEGF. **A:** Representative images of brain sections near the needle track in the high-dose AAV-VEGF group. Vessels are shown in white. **B:** Representative images of brain sections used for vessel quantifications. Dysplastic vessels are indicated by *asterisks*. Bar = 50  $\mu$ m. **C:** Quantification of vessel density. **D:** Quantification of dysplasia index. There were 10 mice in the low-dose AAV-VEGF group and 9 in the high-dose AAV-VEGF group.

we had selected ( $p = 0.63$ ). Similarly, we were not able to detect a difference in the dysplasia index (vessels  $> 15$  mm/200 vessels) between low-dose ( $8.7 \pm 2.1$ ) and high-dose ( $9.8 \pm 1.3$ ) groups ( $p = 0.19$ , Fig. 2B and D).

#### Increase of AAV-VEGF Dose Exacerbated Hemorrhage in bAVM Lesions and Increased Mouse Mortality

To analyze bAVM hemorrhage, iron deposition in bAVMs was quantified using sections stained by Prussian blue. The severity of bAVM hemorrhage was calculated as the percentage of the Prussian blue–positive area over the total area of the ipsilateral hemisphere. Due to the skewed nature of the Prussian blue–positive area, the data observations were log-transformed prior to the analysis. The results showed that bAVMs in the high-dose AAV-VEGF groups have larger Prussian blue–positive areas ( $2.0 \pm 0.3$ )

compared to those in the low-dose AAV-VEGF groups ( $1.4 \pm 0.7$ ;  $p = 0.002$ , Fig. 3).

The overall mortality in the high-dose AAV-VEGF group was 26.7% (4/15) during the follow-up of 8–9 weeks after model induction. No mouse in the low-dose groups died during the same period (OR 9.0, 95% CI 0.4–187.1).

#### VH Exacerbated bAVM Hemorrhage and Increased Mortality

The abnormal vessels in human bAVMs are exposed to varying degrees of increased intraluminal flow and VH. To study whether VH exacerbates bAVM phenotype severity, we created VH in mice 6 weeks after bAVM model induction in a group of low-dose AAV-VEGF–treated mice. As we have demonstrated before,<sup>13,40</sup> the sagittal sinus pressure increased 4- to 6-fold (approximately 8 mm

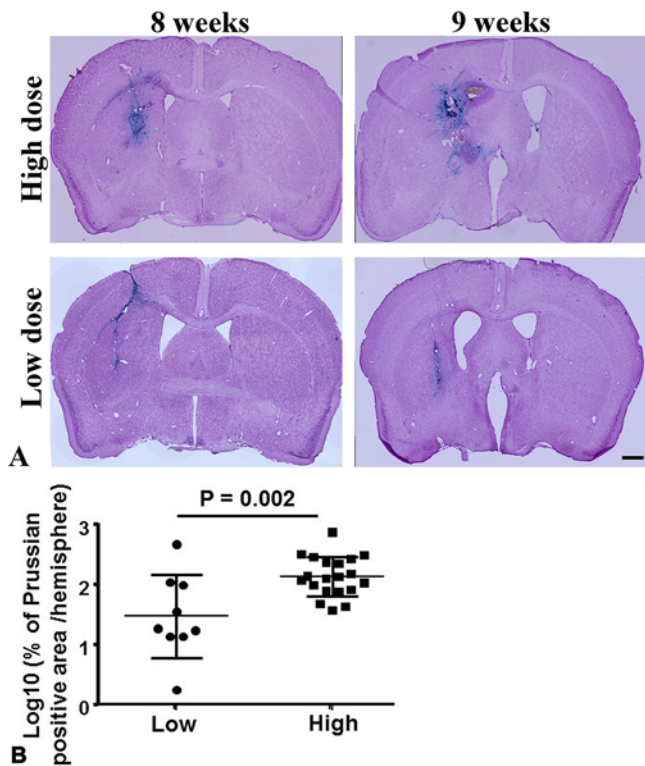


**FIG. 3.** Elevation of the AAV-VEGF dose increased bAVM hemorrhage. **A:** Representative images of Prussian blue–stained sections. The iron depositions (*blue*) in bAVMs indicate hemorrhage. The nuclei were counterstained with Fast Red. Bar = 1 mm. **B:** Quantification of Prussian blue–positive area. Log<sub>10</sub>: the data were 10 log-transformed. Numbers in subgroups were as follows: n = 9 for low-dose AAV-VEGF group and n = 20 for high-dose VEGF group. Figure is available in color online only.

Hg) immediately after the anastomosis of the CCA and the EJV, and was sustained for up to 2 weeks. Brain samples were collected 2 weeks after VH. We found massive hemorrhage in the bAVM lesions of mice subjected to VH (Fig. 4). VH also caused some microhemorrhages in the angiogenic region of the wild-type (WT) brain. VH did not cause hemorrhage in the brain of mice injected with Ad-Cre and AAV-LacZ. Therefore, deletion of *Alkl1* alone or injection of AAV vector does not cause brain hemorrhage. VH increased mortality of bAVM mice; 50% of mice in the bAVM VH group (3 of 6 mice) died before the end of the experiment. Only 1 mouse died in the control group treated with low-dose AAV-VEGF and Ad-GFP (no *Alkl1* deletion, no bAVM) and VH (Fig. 5).

## Discussion

Excessive VEGF expression appears to play an important role in bAVM pathophysiology.<sup>4</sup> In this study, using a mouse bAVM model, we demonstrated that an increase of brain VEGF level through either increasing AAV-VEGF dose or creating cerebral VH exacerbates bAVM hemorrhage and increases mortality.

VEGF expression in the brain is high during embryonic development and is reduced in the adult brain.<sup>32</sup> VEGF expression is higher in surgically resected bAVM lesions compared to normal brain tissue.<sup>17,18,22</sup> Our previous studies showed that VEGF stimulation is necessary for induction of AVM formation in the brains of adult mice.<sup>6,7,38</sup> Blocking VEGF signaling through bevacizumab (an anti-human VEGF antibody) treatment or overexpression of sFLT1 (the extracellular domain of VEGF receptor 1, a soluble form of the VEGF receptor 1) reduces bAVM severity.<sup>39,42,43</sup> All of these data support the notion that VEGF plays an important role in bAVM pathogenesis.

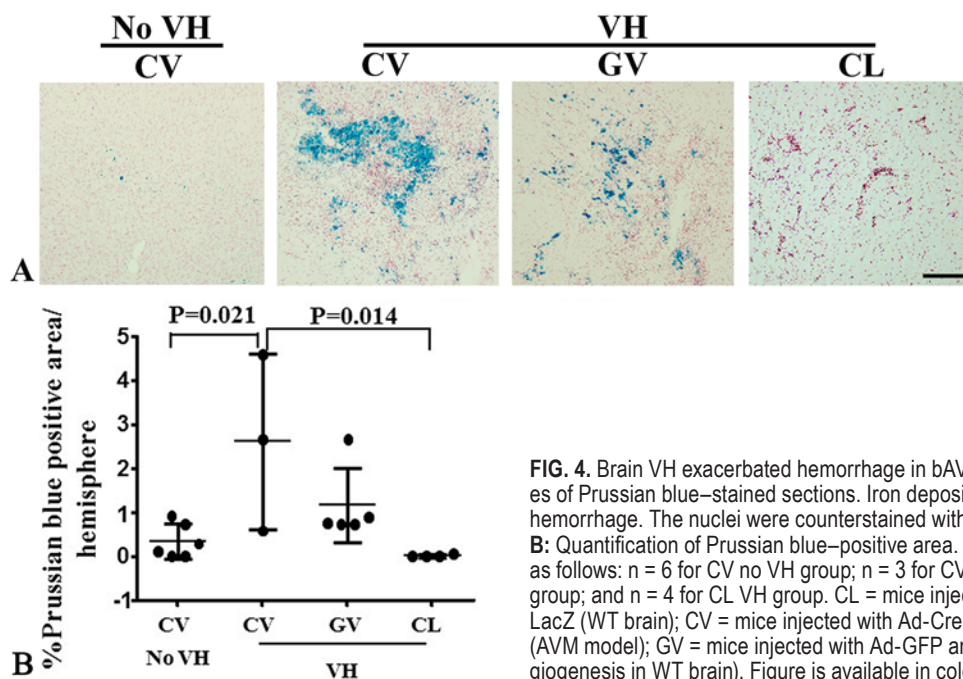


**FIG. 4.** Brain VH exacerbated hemorrhage in bAVMs. **A:** Representative images of Prussian blue–stained sections. Iron depositions (*blue*) in bAVMs indicate hemorrhage. The nuclei were counterstained with Fast Red. Bar = 100  $\mu$ m. **B:** Quantification of Prussian blue–positive area. Numbers in subgroups were as follows: n = 6 for CV no VH group; n = 3 for CV VH group; n = 5 for GV VH group; and n = 4 for CL VH group. CL = mice injected with Ad-GFP and AAV-LacZ (WT brain); CV = mice injected with Ad-Cre and low-dose AAV-VEGF (AVM model); GV = mice injected with Ad-GFP and low-dose AAV-VEGF (angiogenesis in WT brain). Figure is available in color online only.

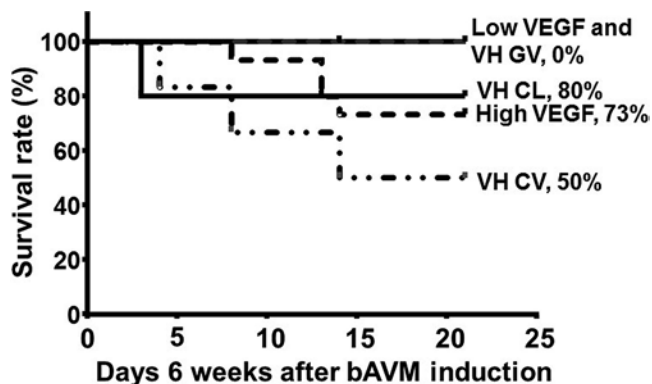


**FIG. 5.** Survival curve. The 0 on the x-axis means the first day of week 7 after model induction. Numbers in subgroups were as follows:  $n = 15$  for high-dose VEGF group;  $n = 11$  for low-dose VEGF group;  $n = 6$  for VH CV group;  $n = 6$  for VH GV group; and  $n = 5$  for VH CL group. CL = mice injected with Ad-GFP and AAV-LacZ (WT brain); CV = mice injected with Ad-Cre and low-dose AAV-VEGF (AVM model); GV = mice injected with Ad-GFP and low-dose AAV-VEGF (angiogenesis in WT brain).

Therefore, blocking VEGF signaling could be a promising strategy to reduce bAVM hemorrhage in patients.

Partial obliteration of bAVM increases the VEGF level in bAVM, which is associated with a high hemorrhage rate;<sup>37</sup> these findings suggest that elevation of VEGF is associated with bAVM hemorrhage. In the present study, using mouse bAVM models, we provide direct evidence to support the notion that an increase of the VEGF level exacerbates bAVM hemorrhage. A significant number of mice in the high-dose AAV-VEGF group died between the 7th and 8th weeks after bAVM induction.

Certain angioarchitecture and corresponding hemodynamic features of bAVM are associated with bAVM hemorrhage, and secondary VEGF elevation might be one of the underlying causes. Our group identified a prolonged venous drainage time in ruptured bAVMs compared to the unruptured lesions.<sup>3</sup> We also found that bAVMs with restricted venous outflow and unbalanced high inflow have a higher future hemorrhage risk.<sup>23</sup> These clinical findings suggest that a restricted venous drainage and accompanying VH might enhance bAVM hemorrhage. VH could induce VEGF expression. In animal models, VH increases brain VEGF expression.<sup>13,44</sup> In *Alkl*-deficient mouse brains, increased focal tissue perfusion and VEGF stimulation have a synergistic effect to promote vascular dysplasia.<sup>15</sup> In this study, we documented that creation of VH in mice with bAVMs caused severe hemorrhage in bAVM lesions and high mortality. The phenotype was similar to what we found in bAVM lesions of mice treated with high-dose AAV-VEGF. Therefore, our data suggest that increased VEGF in response to VH contributes to hemorrhage in bAVM lesions. This might be one of the underlying causes of increased hemorrhage risk in patients with bAVMs with draining vein stenosis or exclusively deep venous drainage, which causes restricted venous drainage and concurrent VH.

Intracranial hemorrhage with an obvious hematoma is the most common presentation in patients with bAVM. Silent intralesional hemorrhage has been found in 30% of

unruptured bAVMs.<sup>14</sup> Conditional deletion of *Alkl* during the embryo development stage resulted in bAVM developing spontaneously, which is accompanied with severe intracranial hemorrhage.<sup>25,29</sup> Most mice died shortly after birth. However, the hemorrhagic phenotype in the *Alkl*-deficient adult bAVM model is less severe.<sup>5</sup> We have previously shown that deletion of the *Itgb8* gene with *Alkl* exacerbated bAVM hemorrhage in our adult mouse model.<sup>24</sup> Therefore, in addition to elevation of VEGF, abnormalities in other genes functioning in angiogenesis may also play a role in bAVM hemorrhage.

### Study Limitations

There are several limitations of this study, as follows.

- 1) The vessel density and the number of dysplastic vessels were not quantified properly in the brains of the high-dose AAV-VEGF group due to the severe hemorrhage. For these brains, we had to select sections farther away from the injection site for vessel quantification. Therefore, the vessel density and the number of dysplastic vessels in the high-dose AAV-VEGF group were underestimated. We were not able to show the differences between high- and low-dose AAV-VEGF groups.
- 2) Due to the extremely high mortality in the low-dose AAV-VEGF/VH group, we did not add more mice to measure VEGF expression in this study. We showed in our previous studies that VH increases VEGF expression in mouse and rat brain.<sup>13,44</sup> The mice used in this study had the same strain/type as the mice we used in our previous study;<sup>13</sup> they were all in C57BL/6J background. Even though all conditions used in this study were the same as those used in our previous investigation, the mice in the current study may not have had the same level of VEGF in their brains as in the previous study.
- 3) We have tested anti-VEGF therapies previously and have shown the following: bevacizumab treatment inhibits bAVM formation and progression,<sup>39</sup> which has led to a clinical trial at UCSF (ClinicalTrials.gov, NCT02314377); and intravenous injection of AAV-sFLT1 attenuates the severity of bAVM phenotypes.<sup>43</sup> Unfortunately, we did not analyze hemorrhage in these studies. We will do so in future studies.
- 4) In this study, we used the AAV vector to overexpress exogenous VEGF chronically to demonstrate that increasing the VEGF level chronically before and after bAVM formation increases bAVM hemorrhage. We have also created VH in mice in which bAVM is still developing to test if an increase of venous pressure increases bAVM hemorrhage. However, these models may not completely mimic the clinical scenario, because a surge of VEGF level, increases of other angiogenic factors, and changes of hemodynamics other than VH may contribute to bAVM hemorrhage.
- 5) In addition to increasing the VEGF level in the brain, VH also increased the pressure in the brain venous system and the sagittal sinus. VH also increased inflammatory factors, such as matrix metalloproteinase (MMP9) activity and leukocyte infiltration.<sup>13,44</sup> Therefore, VH can increase bAVM hemorrhage through other mechanisms.

6) Because increasing the AAV-VEGF dose elevated exogenous VEGF level in the bAVM lesion, to demonstrate that an increase of endogenous VEGF can also increase bAVM hemorrhage, we created VH in mice with bAVMs, because VH can increase the endogenous VEGF level in the brain.<sup>13,44</sup> As shown in Fig. 4, VH significantly increased bAVM hemorrhage and mortality. However, due to the high mortality rate (50%), we did not induce VH in more mice with bAVMs. Therefore, the sample size in this study is small.

## Conclusions

In this paper, we provided direct evidence that elevation of the VEGF level increases bAVM hemorrhage and mortality in a mouse bAVM model. Therefore, inhibition of VEGF might be a promising strategy to prevent bAVM hemorrhage or reduce the severity of hemorrhage.

## Acknowledgments

This study was supported by grants to Dr. Su from the NIH (R01 NS027713 and R01 HL122774) and the Michael Ryan Zodda Foundation; a grant to Dr. Walker from NIH T32 (GM008440); and a fellowship to Mr. Cheng from the Foundation of Anesthesia Education and Research.

## References

- Al-Shahi Salman R, White PM, Counsell CE, du Plessis J, van Beijnum J, Josephson CB, et al: Outcome after conservative management or intervention for unruptured brain arteriovenous malformations. **JAMA** **311**:1661–1669, 2014
- Avery RL, Pearlman J, Pieramici DJ, Rabena MD, Castellarin AA, Nasir MA, et al: Intravitreal bevacizumab (Avastin) in the treatment of proliferative diabetic retinopathy. **Ophthalmology** **113**:1695.e1–1695.e15, 2006
- Burkhardt JK, Chen X, Winkler EA, Cooke DL, Kim H, Lawton MT: Delayed venous drainage in ruptured arteriovenous malformations based on quantitative color-coded digital subtraction angiography. **World Neurosurg** **104**:619–627, 2017
- Chen W, Choi EJ, McDougall CM, Su H: Brain arteriovenous malformation modeling, pathogenesis, and novel therapeutic targets. **Transl Stroke Res** **5**:316–329, 2014
- Chen W, Guo Y, Walker EJ, Shen F, Jun K, Oh SP, et al: Reduced mural cell coverage and impaired vessel integrity after angiogenic stimulation in the Alk1-deficient brain. **Arterioscler Thromb Vasc Biol** **33**:305–310, 2013
- Chen W, Sun Z, Han Z, Jun K, Camus M, Wankhede M, et al: De novo cerebrovascular malformation in the adult mouse after endothelial Alk1 deletion and angiogenic stimulation. **Stroke** **45**:900–902, 2014
- Choi EJ, Chen W, Jun K, Arthur HM, Young WL, Su H: Novel brain arteriovenous malformation mouse models for type 1 hereditary hemorrhagic telangiectasia. **PLoS One** **9**:e88511, 2014
- Choi EJ, Walker EJ, Degos V, Jun K, Kuo R, Pile-Spellman J, et al: Endoglin deficiency in bone marrow is sufficient to cause cerebrovascular dysplasia in the adult mouse after vascular endothelial growth factor stimulation. **Stroke** **44**:795–798, 2013
- Choi EJ, Walker EJ, Shen F, Oh SP, Arthur HM, Young WL, et al: Minimal homozygous endothelial deletion of Eng with VEGF stimulation is sufficient to cause cerebrovascular dysplasia in the adult mouse. **Cerebrovasc Dis** **33**:540–547, 2012
- Cockroft KM, Jayaraman MV, Amin-Hanjani S, Derdeyn CP, McDougall CG, Wilson JA: A perfect storm: how a randomized trial of unruptured brain arteriovenous malformations' (ARUBA's) trial design challenges notions of external validity. **Stroke** **43**:1979–1981, 2012
- Derdeyn CP, Zipfel GJ, Albuquerque FC, Cooke DL, Feldmann E, Sheehan JP, et al: Management of brain arteriovenous malformations: a scientific statement for healthcare professionals from the American Heart Association/American Stroke Association. **Stroke** **48**:e200–e224, 2017
- Fleetwood IG, Steinberg GK: Arteriovenous malformations. **Lancet** **359**:863–873, 2002
- Gao P, Zhu Y, Ling F, Shen F, Lee B, Gabriel RA, et al: Non-ischemic cerebral venous hypertension promotes a pro-angiogenic stage through HIF-1 downstream genes and leukocyte-derived MMP-9. **J Cereb Blood Flow Metab** **29**:1482–1490, 2009
- Guo Y, Saunders T, Su H, Kim H, Akkoc D, Saloner DA, et al: Silent intralesional microhemorrhage as a risk factor for brain arteriovenous malformation rupture. **Stroke** **43**:1240–1246, 2012
- Hao Q, Su H, Marchuk DA, Rola R, Wang Y, Liu W, et al: Increased tissue perfusion promotes capillary dysplasia in the ALK1-deficient mouse brain following VEGF stimulation. **Am J Physiol Heart Circ Physiol** **295**:H2250–H2256, 2008
- Hao Q, Zhu Y, Su H, Shen F, Yang GY, Kim H, et al: VEGF induces more severe cerebrovascular dysplasia in Endoglin<sup>+</sup> than in Alk1<sup>+</sup> mice. **Transl Stroke Res** **1**:197–201, 2010
- Hashimoto T, Emala CW, Joshi S, Mesa-Tejada R, Quick CM, Feng L, et al: Abnormal pattern of Tie-2 and vascular endothelial growth factor receptor expression in human cerebral arteriovenous malformations. **Neurosurgery** **47**:910–919, 2000
- Hashimoto T, Wu Y, Lawton MT, Yang GY, Barbaro NM, Young WL: Coexpression of angiogenic factors in brain arteriovenous malformations. **Neurosurgery** **56**:1058–1065, 2005
- Kashiwazaki D, Kobayashi R, Houkin K, Kuroda S: Increased expression of vascular endothelial growth factor and its receptor in enlarging brain arteriovenous malformations—a case report. **Br J Neurosurg** **28**:119–121, 2014
- Kiliç T, Pamir MN, Küllü S, Eren F, Ozek MM, Black PM: Expression of structural proteins and angiogenic factors in cerebrovascular anomalies. **Neurosurgery** **46**:1179–1192, 2000
- Kim H, Pawlikowska L, Young WL: Genetics and vascular biology of brain vascular malformations (Chapter 12), in Mohr JP, Wolf PA, Grotta JC, et al (eds): **Stroke: Pathophysiology, Diagnosis, and Management**, ed 5. Philadelphia: Churchill Livingstone Elsevier, 2011, pp 169–186
- Koizumi T, Shiraishi T, Hagihara N, Tabuchi K, Hayashi T, Kawano T: Expression of vascular endothelial growth factors and their receptors in and around intracranial arteriovenous malformations. **Neurosurgery** **50**:117–126, 2002
- Ma L, Chen XL, Chen Y, Wu CX, Ma J, Zhao YL: Subsequent haemorrhage in children with untreated brain arteriovenous malformation: Higher risk with unbalanced inflow and outflow angioarchitecture. **Eur Radiol** **27**:2868–2876, 2017
- Ma L, Shen F, Jun K, Bao C, Kuo R, Young WL, et al: Integrin  $\beta 8$  deletion enhances vascular dysplasia and hemorrhage in the brain of adult Alk1 heterozygous mice. **Transl Stroke Res** **7**:488–496, 2016
- Milton I, Seki T: Transgenic mouse model of hemorrhagic arteriovenous malformation in brain and spinal cord. **Stroke** **42**:e91, 2011 (Abstract #163)
- Mohr JP, Moskowitz AJ, Parides M, Stapf C, Young WL: Hull down on the horizon: A Randomized trial of Unruptured Brain Arteriovenous malformations (ARUBA) trial. **Stroke** **43**:1744–1745, 2012



27. Mohr JP, Moskowitz AJ, Stapf C, Hartmann A, Lord K, Marshall SM, et al: The ARUBA trial: current status, future hopes. **Stroke** **41**:e537–e540, 2010
28. Mohr JP, Parides MK, Stapf C, Moquete E, Moy CS, Overbey JR, et al: Medical management with or without interventional therapy for unruptured brain arteriovenous malformations (ARUBA): a multicentre, non-blinded, randomised trial. **Lancet** **383**:614–621, 2014
29. Park SO, Lee YJ, Seki T, Hong KH, Fliess N, Jiang Z, et al: ALK5- and TGFBR2-independent role of ALK1 in the pathogenesis of hereditary hemorrhagic telangiectasia type 2. **Blood** **111**:633–642, 2008
30. Shen F, Su H, Liu W, Kan YW, Young WL, Yang GY: Recombinant adeno-associated viral vector encoding human VEGF165 induces neomicrovessel formation in the adult mouse brain. **Front Biosci** **11**:3190–3198, 2006
31. Shen F, Walker EJ, Jiang L, Degos V, Li J, Sun B, et al: Co-expression of angiopoietin-1 with VEGF increases the structural integrity of the blood-brain barrier and reduces atrophy volume. **J Cereb Blood Flow Metab** **31**:2343–2351, 2011
32. Sonstein WJ, Kader A, Michelsen WJ, Llena JF, Hirano A, Casper D: Expression of vascular endothelial growth factor in pediatric and adult cerebral arteriovenous malformations: an immunocytochemical study. **J Neurosurg** **85**:838–845, 1996
33. Spaide RF, Laud K, Fine HF, Klanck JM Jr, Meyerle CB, Yannuzzi LA, et al: Intravitreal bevacizumab treatment of choroidal neovascularization secondary to age-related macular degeneration. **Retina** **26**:383–390, 2006
34. Stapf C, Mohr JP, Choi JH, Hartmann A, Mast H: Invasive treatment of unruptured brain arteriovenous malformations is experimental therapy. **Curr Opin Neurol** **19**:63–68, 2006
35. Su H, Lu R, Kan YW: Adeno-associated viral vector-mediated vascular endothelial growth factor gene transfer induces neovascular formation in ischemic heart. **Proc Natl Acad Sci U S A** **97**:13801–13806, 2000
36. Sure U, Butz N, Schlegel J, Siegel AM, Wakat JP, Mennel HD, et al: Endothelial proliferation, neoangiogenesis, and potential de novo generation of cerebrovascular malformations. **J Neurosurg** **94**:972–977, 2001
37. van Beijnum J, van der Worp HB, Buis DR, Al-Shahi Salman R, Kappelle LJ, Rinkel GJ, et al: Treatment of brain arteriovenous malformations: a systematic review and meta-analysis. **JAMA** **306**:2011–2019, 2011
38. Walker EJ, Su H, Shen F, Choi EJ, Oh SP, Chen G, et al: Arteriovenous malformation in the adult mouse brain resembling the human disease. **Ann Neurol** **69**:954–962, 2011
39. Walker EJ, Su H, Shen F, Degos V, Amend G, Jun K, et al: Bevacizumab attenuates VEGF-induced angiogenesis and vascular malformations in the adult mouse brain. **Stroke** **43**:1925–1930, 2012 (Erratum in **Stroke** **44**:e21, 2013)
40. Yang ST, Rodriguez-Hernandez A, Walker EJ, Young WL, Su H, Lawton MT: Adult mouse venous hypertension model: common carotid artery to external jugular vein anastomosis. **J Vis Exp** **95**:e50472, 2015
41. Zhang ZG, Zhang L, Jiang Q, Zhang R, Davies K, Powers C, et al: VEGF enhances angiogenesis and promotes blood-brain barrier leakage in the ischemic brain. **J Clin Invest** **106**:829–838, 2000
42. Zhu W, Shen F, Kang S, et al: Soluble FLT1 gene therapy through systemic viral delivery reduces the severity of mouse brain arteriovenous malformation. **Stroke** **47** (Suppl 1):A54, 2016 (Abstract)
43. Zhu W, Shen F, Mao L, Zhan L, Kang S, Sun Z, et al: Soluble FLT1 gene therapy alleviates brain arteriovenous malformation severity. **Stroke** **48**:1420–1423, 2017
44. Zhu Y, Lawton MT, Du R, Shwe Y, Chen Y, Shen F, et al: Expression of hypoxia-inducible factor-1 and vascular endothelial growth factor in response to venous hypertension. **Neurosurgery** **59**:687–696, 2006

---

### Disclosures

The authors report no conflict of interest concerning the materials or methods used in this study or the findings specified in this paper.

### Author Contributions

Conception and design: Su, Cheng, Ma, Walker. Acquisition of data: Cheng, Ma, Shaligram, Walker, Yang, Tang, W Zhu, Zhan, Li, X Zhu. Analysis and interpretation of data: Su, Cheng, Ma, Shaligram, Walker, Yang, Tang, W Zhu, Zhan, Li, X Zhu. Drafting the article: Su, Ma. Critically revising the article: Su, Walker, Lawton. Reviewed submitted version of manuscript: Su. Approved the final version of the manuscript on behalf of all authors: Su. Statistical analysis: Cheng, Ma, Shaligram. Administrative/technical/material support: Su, Lawton. Study supervision: Su.

### Supplemental Information

#### Current Affiliations

Dr. Lawton: Barrow Neurological Institute, Phoenix, AZ.

### Correspondence

Hua Su: University of California, San Francisco, CA. hua.su@ucsf.edu.